Definitive Determination of Zero-Field Splitting and Exchange Interactions in a Ni(II) Dimer: Investigation of [Ni$_2$(en)$_4$Cl$_2$]Cl$_2$ Using Magnetization and Tunable-Frequency High-Field Electron Paramagnetic Resonance

Radovan Herchel,*,[†] Roman Boča,[‡] J. Krzystek,[§] Andrew Ozarowski,[§] Marc Durán,[#] and Joris van Slageren[#]

Department of Inorganic Chemistry, Palacký University, CZ-77147 Olomouc, Czech Republic, Institute of Inorganic Chemistry, Slovak Technical University, SK-812 37 Bratislava, Slovakia, National High Magnetic Field Laboratory, Florida State University, Tallahassee, Florida 32310, and 1. Physikalisches Institut, Universität Stuttgart, Pfaffenwaldring 57, D-70550 Stuttgart, Germany

Received April 13, 2007; E-mail: radovan.herchel@upol.cz

Understanding the origin of zero-field splitting (ZFS) in molecular magnets is of great importance, because the ZFS determines many of their interesting properties, such as magnetic hysteresis and quantum tunneling of the magnetization.[1]

The aim of this report is to elucidate the microscopic origin of ZFS in dinuclear exchange coupled systems with large anisotropies. To this end we have prepared a nickel(II) complex bis(μ-chloro)-tetrakis(ethylenediamine)dinickel(II) dichloride, [Ni$_2$(en)$_4$Cl$_2$]Cl$_2$ (**1**) (Figure 1).[2]

Several sets of spin Hamiltonian parameters have been published for **1** (Table 1), all obtained from temperature-dependent magnetic susceptibility; they are not in agreement. We have investigated **1** in detail using both magnetization and magnetic resonance measurements and are now able to unambiguously determine these parameters 35 years after the first attempt. This shows the effectiveness of magnetic resonance techniques at obtaining reliable ZFS parameters. An additional reason for the failure of magnetometry to deliver accurate spin Hamiltonian values, particularly ZFS, is the often used strong exchange approximation. This approximation assumes the isotropic exchange to be much stronger than other interactions.

Magnetic properties of **1** are shown in Figure 2.[7] The effective magnetic moment μ_{eff} at $T = 300$ K is 4.6 μ_B. Upon cooling it increases reaching a maximum of 5.1 μ_B at $T = 14.0$ K and then decreases to 3.6 μ_B at $T = 2.0$ K. The initial increase indicates ferromagnetic exchange interactions between the Ni ions, while the decrease at the lowest temperatures can be ascribed to the ZFS of the ground state. The measured value of magnetization at $B = 5.5$ T and low temperatures (Figure 2) indicates a $S = 2$ ground state, for which the theoretical saturation magnetization per complex is $M_{mol}/(N_A\mu_B) = 4.0$ for $g = 2.0$.

To explain the magnetic behavior of **1**, the following spin Hamiltonian was postulated:[8]

$$\hat{H}_a = -J(\vec{S}_A \cdot \vec{S}_B) + D_A(\hat{S}_{Az}^2 - {}^1/_3\vec{S}_A^2) + \\ D_B(\hat{S}_{Bz}^2 - {}^1/_3\vec{S}_B^2) + D_{AB}(\hat{S}_{Az}\hat{S}_{Bz} - {}^1/_3\vec{S}_A \cdot \vec{S}_B) + \\ \mu_B g_a B_a \hat{S}_a - zj\langle S_a \rangle \hat{S}_a \quad (1)$$

where J stands for the isotropic exchange constant, D_A and D_B are the axial single-ion ZFS parameters, D_{AB} is the asymmetric exchange parameter (the sum of dipolar and anisotropic exchange interactions between the two magnetic centers). We assumed that
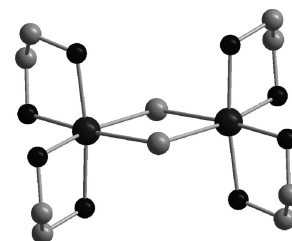
† Palacký University.
‡ Slovak Technical University.
§ Florida State University.
# Universität Stuttgart.

Figure 1. X-ray structure of [Ni$_2$(en)$_4$Cl$_2$]$^{2+}$.[3] Hydrogen atoms are omitted for the sake of clarity.
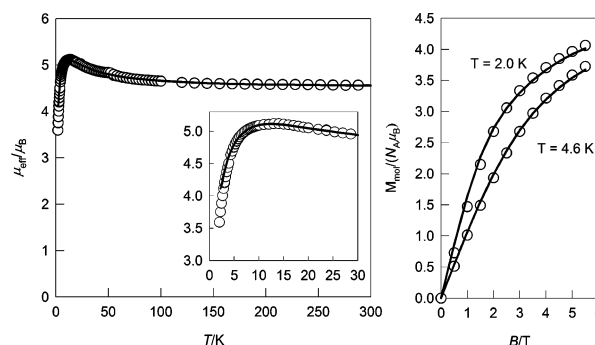

Figure 2. Magnetic properties of **1**: (left) temperature dependence of the effective magnetic moment (calculated from magnetization at $B = 0.1$ T), with the low-T region expanded in the inset; (right) field dependence of magnetization at $T = 2.0$ and 4.6 K. Circles represent experimental points, lines represent calculated values using the best-fit parameters (Table 1).

Table 1. Magnetic Parameters for **1**

parameter[a]	Ginsberg et al.[4]	Ginsberg et al.[4]	Journaux et al.[5]	Joung et al.[6]	this work
J (cm^{-1})	+19.7	+20.9	+5.1	+7.0	+9.66
g_{iso}	2.14	2.12		2.25	2.242
D_A (cm^{-1})	−6.5	+11.1	−10.0	−9.7	−4.78
D_{AB} (cm^{-1})					−0.64
E_A (cm^{-1})			−2.0		
zj (cm^{-1})	−0.33	−0.042		−0.42	−0.402

[a] All values are written according to convention in eq 1.

the principal axis of the local $\mathbf{D_A}$, $\mathbf{D_B}$, and the pairwise $\mathbf{D_{AB}}$ tensors coincide. zj is the common molecular-field parameter which is due to small intermolecular interactions and $\langle S_a \rangle$ is a thermal average of the spin projection in a direction. The assumption of a molecular-field parameter is supported by the existence of the hydrogen-bond network (Supporting Information, Figure S1). The antisymmetric exchange was excluded due to the inversion center in midpoint between Ni(II) centers.
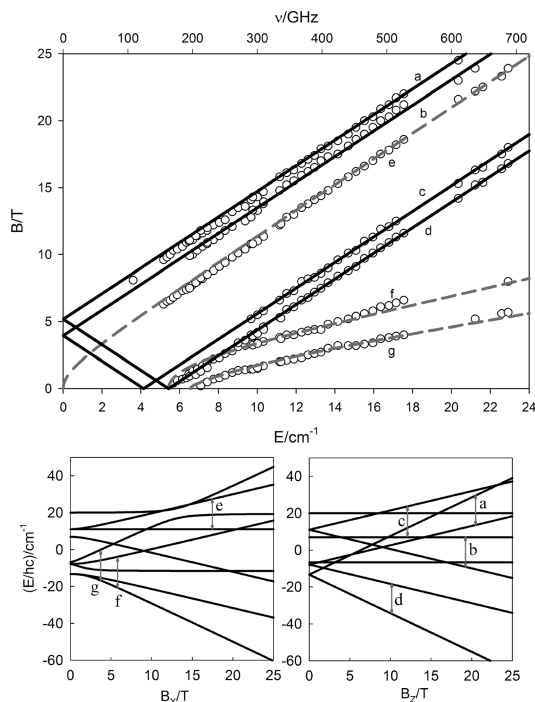
Figure 3. (Top) A plot of HFEPR resonances in **1** vs sub-THz frequency at $T = 4.2$ K. Circles represent experimental resonance positions at specific frequencies; lines represent calculated values using spin Hamiltonian parameters in Table 1 for parallel (black solid line) and perpendicular (gray dashed line) turning points, respectively. (Bottom) Reconstructed energy levels for perpendicular (left) and parallel (right) magnetic field direction. Labels correspond to transitions at $\nu = 500$ GHz: a, transition $|2,+1\rangle \leftrightarrow |2,+2\rangle$; b, transition $|1,-1\rangle \leftrightarrow 1,0\rangle$; c, transition $|1,+1\rangle \leftrightarrow |1,0\rangle$; d, transition $|2,-1\rangle \leftrightarrow |2,-2\rangle$; e, transition $|1,0\rangle \leftrightarrow |1,+1\rangle$; f, transition $|2,-2\rangle \leftrightarrow |2,+1\rangle$; and g, transition $|2,-2\rangle \leftrightarrow |2,+2\rangle$.

For the magnetic field vector in the polar coordinates defined as $\vec{B}_a = B(\sin\theta\cos\varphi, \sin\theta\sin\varphi, \cos\theta)$ the molar magnetization was calculated as

$$M_{a,\mathrm{mol}} = -N_A \frac{\sum_i (\sum_k \sum_l C_{ik}^+ (Z_a)_{kl} C_{li}) \exp(-\epsilon_{a,i}/kT)}{\sum_i \exp(-\epsilon_{a,i}/kT)} \quad (2)$$

where Z_a is the matrix element of Zeeman term for the a direction of the magnetic field and C are the eigenvectors resulting from the diagonalization of the complete spin Hamiltonian matrix.

Since a powder sample was used, the averaged molar magnetization was calculated as an orientational average

$$M_{\mathrm{mol}} = {}^\pi/_4 \int_0^{2\pi} \int_0^\pi M_{a,\mathrm{mol}} \sin\theta \, d\theta \, d\varphi \quad (3)$$

There are five adjustable parameters in Hamiltonian (1): J, g, D_A (equal to D_B by symmetry), D_{AB} and zj. All five cannot be obtained reliably from fitting the magnetization data alone and therefore tunable-frequency high-field EPR measurements[9] were performed. The recorded EPR transitions together with all magnetization data were handled by an advanced fitting procedure,[10] the results of which are collected in Table 1, Figures 2 and 3.

The sign of D_A and D_{AB} was determined by a temperature dependence of EPR spectra at 350 GHz (Figure S2). The absorption peak at $B = 6$ T is assigned to a parallel transition in the lowest quintet $|2,-2\rangle \leftrightarrow |2,-1\rangle$ and its intensity is increasing on lowering the temperature, which is in agreement with simulated ideal powder

spectra for the best-fitted parameters using the EasySpin package.[11] Further, experimental and simulated powder HFEPR spectra at various frequencies (Figure S3) show good conformity.

The values of both anisotropy parameters of interest: local (single-ion) $D_A = -4.78$ cm^{-1} and pairwise (asymmetric) $D_{AB} = -0.64$ cm^{-1} were thus found. A moderate positive value of the exchange coupling constant $J = +9.66$ cm^{-1}, when compared with D_A, means that the condition of strong exchange coupling is no longer fulfilled.

The reconstructed energy levels calculated using magnetic parameters in Table 1 are displayed in Figure 3. ZFS parameters calculated for molecular spin states by using coupling coefficients[8] are $D_1 = (-D_A + D_{AB}) = +4.1$ cm^{-1} for $S = 1$ and $D_2 = (D_A + D_{AB})/3 = -1.8$ cm^{-1} for $S = 2$. In the weak exchange limit (Figure S4), the two molecular spin states $|2, 0\rangle$ and $|0, 0\rangle$ are mixed through ZFS interaction and the energy gap between $|2, 0\rangle$ and $|2, \pm1\rangle$ is not equal to D_2 but has a value of $\Delta_2 = -1.1$ cm^{-1}.

In conclusion, our declared goal to determine reliably all spin Hamiltonian parameters in **1** was accomplished. To our best knowledge, this is the first time that the D_{AB} parameter was extracted from a powder sample of a Ni(II) dinuclear complex using modern magnetic and spectroscopic techniques cooperatively. The information thus acquired, together with the methodology developed to this purpose, will enhance our understanding of the properties of more complicated metal clusters. In particular, it will allow one to relate the experimental observables to microscopic interactions in such systems.

Supporting Information Available: Details of synthesis, H-bond network formation in **1**, EPR spectra at different temperatures and frequencies, energy level mixing in the weak exchange limit. This material is available free of charge via the Internet at http://pubs.acs.org.

References

(1) (a) Sessoli, R.; Gatteschi, D.; Caneschi, A.; Novak, M. A. *Nature* **1993**, *365*, 141−143. (b) McInnes, E. J. L. In *Single-Molecule Magnets and Related Phenomena;* Springer: Berlin, 2006; Vol. 122, p 69−102.
(2) The compound was prepared according to the following reference and characterized as described in Supporting Information: State, H. M. *Inorg. Synth.* **1960**, *6*, 198.
(3) Bottomley, G. A.; Glossop, L. G.; Skelton, B. W.; White, A. H. *Aust. J. Chem*. **1979**, *32*, 285−289.
(4) Ginsberg, A. P.; Brookes, R. W.; Martin, R. L.; Sherwood, R. C. *Inorg. Chem*. **1972**, *11*, 2884−2889.
(5) Journaux, Y.; Kahn, O.; Chevalier, B.; Etourneau, J.; Claude, R.; Dworkin, A. *Chem. Phys. Lett.* **1978**, *55*, 140−143.
(6) Joung, K. O.; O'Connor, C. J.; Sinn, E.; Carlin, R. L. *Inorg. Chem.* **1979**, *18*, 804−808.
(7) The magnetization was measured using SQUID magnetometer (Quantum Design) at 0.1 T between 2 and 300 K and its field dependence up to 5.5 T at 2.0 and 4.6 K. A correction to the underlying diamagnetism was estimated on the basis of Pascal constants as $\chi_{dia} = -3.9 \times 10^{-9}$ m^3 mol^{-1}. Tunable-frequency high-field EPR was performed in a 150−700 GHz frequency range using the mm and sub-mm wave facility and the 25-T resistive "Keck" magnet at NHMFL and in a 150−800 GHz range using a 7-T split-coil superconducting magnet at Universität Stuttgart.
(8) Boča, R. *Theoretical Foundations of Molecular Magnetism*; Elsevier: Amsterdam, 1999.
(9) Krzystek, J.; Zvyagin, S. A.; Ozarowski, A.; Trofimenko, S.; Telser, J. *J. Magn. Reson.* **2006**, *178*, 174−183.
(10) Calculation and fitting details are summarized in the Supporting Information.
(11) Stoll, S.; Schweiger, A. *J. Magn. Reson.* **2006**, *178*, 42−55.

JA0725807